New Middle Pleistocene hominin cranium from Gruta da Aroeira (Portugal)

Joan Daura[a], Montserrat Sanz[b,c], Juan Luis Arsuaga[b,c,1], Dirk L. Hoffmann[d], Rolf M. Quam[c,e,f], María Cruz Ortega[b,c], Elena Santos[b,c,g], Sandra Gómez[h], Angel Rubio[i], Lucía Villaescusa[h], Pedro Souto[j,k], João Mauricio[j,k], Filipa Rodrigues[j,k], Artur Ferreira[j], Paulo Godinho[j], Erik Trinkaus[l], and João Zilhão[a,m,n]

[a]UNIARQ-Centro de Arqueologia da Universidade de Lisboa, Faculdade de Letras, Universidade de Lisboa, 1600-214 Lisbon, Portugal; [b]Departamento de Paleontología, Facultad de Ciencias Geológicas, Universidad Complutense de Madrid, 28040 Madrid, Spain; [c]Centro Universidad Complutense de Madrid-Instituto de Salud Carlos III de Investigación sobre la Evolución y Comportamiento Humanos, 28029 Madrid, Spain; [d]Department of Human Evolution, Max Planck Institute for Evolutionary Anthropology, 04103 Leipzig, Germany; [e]Department of Anthropology, Binghamton University-State University of New York, Binghamton, NY 13902; [f]Division of Anthropology, American Museum of Natural History, New York, NY 10024; [g]Laboratorio de Evolución Humana, Universidad de Burgos, 09001 Burgos, Spain; [h]Grup de Recerca del Quaternari - Seminari d'Estudis i Recerques Prehistòriques, Department of History and Archaeology, University of Barcelona, 08007 Barcelona, Spain; [i]Laboratorio de Antropología, Departamento de Medicina Legal, Toxicología y Antropología Física, Facultad de Medicina, Universidad de Granada, 18010 Granada, Spain; [j]Crivarque - Estudos de Impacto e Trabalhos Geo-Arqueológicos Lda, 2350 Torres Novas, Portugal; [k]Sociedade Torrejana de Espeleologia e Arqueologia, 2350 Torres Novas Portugal; [l]Department of Anthropology, Washington University in Saint Louis, Saint Louis, MO 63130; [m]Department of History and Archaeology, University of Barcelona, 08007 Barcelona, Spain; and [n]Catalan Institution for Research and Advanced Studies, 08010 Barcelona, Spain

Contributed by Juan Luis Arsuaga, January 27, 2017 (sent for review November 21, 2016; reviewed by William Henry Gilbert and Giorgio Manzi)

The Middle Pleistocene is a crucial time period for studying human evolution in Europe, because it marks the appearance of both fossil hominins ancestral to the later Neandertals and the Acheulean technology. Nevertheless, European sites containing well-dated human remains associated with an Acheulean toolkit remain scarce. The earliest European hominin crania associated with Acheulean handaxes are at the sites of Arago, Atapuerca Sima de los Huesos (SH), and Swanscombe, dating to 400–500 ka (Marine Isotope Stage 11–12). The Atapuerca (SH) fossils and the Swanscombe cranium belong to the Neandertal clade, whereas the Arago hominins have been attributed to an incipient stage of Neandertal evolution, to *Homo heidelbergensis*, or to a subspecies of *Homo erectus*. A recently discovered cranium (Aroeira 3) from the Gruta da Aroeira (Almonda karst system, Portugal) dating to 390–436 ka provides important evidence on the earliest European Acheulean-bearing hominins. This cranium is represented by most of the right half of a calvarium (with the exception of the missing occipital bone) and a fragmentary right maxilla preserving part of the nasal floor and two fragmentary molars. The combination of traits in the Aroeira 3 cranium augments the previously documented diversity in the European Middle Pleistocene fossil record.

human evolution | Neandertal roots | evolutionary patterns | Acheulean | Europe

The Gruta da Aroeira Site

Ongoing research and excavations since 1987 at the Almonda cluster of paleoanthropological localities in central Portugal (Fig. 1, Fig. S1, and *SI The Gruta da Aroeira Site*) have yielded human remains and rich archaeological levels of the Lower, Middle, and Upper Paleolithic as well as Early Neolithic and later prehistoric periods (1–12). Within the Almonda karst system, the Gruta da Aroeira was first investigated from 1998–2002 (13), revealing a rich lithic assemblage with Acheulean bifaces (Fig. S2) associated with faunal remains and two human teeth (Fig. S3): Aroeira 1 (a left mandibular canine) and Aroeira 2 (a left maxillary third molar). Aroeira 1 is moderately large, especially compared with the Atapuerca (SH) sample, and Aroeira 2 is among the larger of the Middle Pleistocene upper right third molars (6, 14). They fit morphologically within the known variation of European Middle Pleistocene dentitions, although Aroeira 2 has a relatively large hypocone (6, 15).

Renewed fieldwork in 2013, focused on establishing the chronology of the sequence via U-series dating of interstratified flowstone deposits (Figs. 1 and 2), led to the discovery of a human cranium (Aroeira 3) encased in hard breccia toward the base of the sequence (Fig. 3 and Fig. S4).

The Aroeira stratigraphy spans a thickness of ∼4 m and comprises three major stratigraphic units (Fig. 2 and *SI Stratigraphic Outline*). The cranium was recovered from unit 2, a 2.2-m-thick mud-supported breccia rich in angular and subangular clasts. This unit corresponds to the Acheulean layer X–Xb/c [the upper and lower parts of a single layer excavated in 1998–2002 (X) and in 2013–2015 (Xb/c)], and the overlying ARO2 flowstone has yielded a minimum age of 417.7 + 37.3/−27.5 ka (*SI U-Series Results* and Table S1) (9). A further uranium-thorium (U-Th) age of 406 ± 30 ka for the outer layer of a stalagmitic column (*SI Chronostratigraphy*) covered by unit 2 provides a maximum age for the sequence and allows correlation of it to Marine Isotope Stage (MIS) 11. Two additional U-Th ages of 390 ± 14 ka and 408 ± 18 ka for calcitic crusts that formed on the cranium provide additional, consistent minimum age constraints for the cranium itself (*SI Chronostratigraphy*). Thus, the Aroeira 3 cranium most likely dates to 390–436 ka.

Our excavation of layer X–Xb/c covered an area of 6 m^2 and a depth of 1 m. The lithic assemblage recovered (n = 387) includes handaxes and other bifacial tools (n = 17), other retouched tools (n = 27), cores (n = 43), flakes or flake fragments and debris (n = 180), and tested or untested cobbles (possibly manuports) (n = 114). Quartzite is

Significance

We describe a recently discovered cranium from the Aroeira cave in Portugal dated to around 400 ka. This specimen is the westernmost Middle Pleistocene cranium of Europe and is one of the earliest fossils from this region associated with Acheulean tools. Unlike most other Middle Pleistocene finds, which are of uncertain chronology, the Aroeira 3 cranium is firmly dated to around 400 ka and was in direct association with abundant faunal remains and stone tools. In addition, the presence of burnt bones suggests a controlled use of fire. The Aroeira cranium represents a substantial contribution to the debate on the origin of the Neandertals and the pattern of human evolution in the Middle Pleistocene of Europe.

Author contributions: J.D., M.S., J.L.A., D.L.H., R.M.Q., E.T., and J.Z. designed research; J.D., M.S., J.L.A., D.L.H., R.M.Q., S.G., A.R., L.V., P.S., J.M., F.R., A.F., P.G., E.T., and J.Z. performed research; J.D., M.S., J.L.A., D.L.H., R.M.Q., M.C.O., E.S., E.T., and J.Z. analyzed data; and J.D., M.S., J.L.A., D.L.H., R.M.Q., M.C.O., E.S., E.T., and J.Z. wrote the paper.

Reviewers: W.H.G., California State University, East Bay; and G.M., Sapienza University of Rome.

The authors declare no conflict of interest.

Freely available online through the PNAS open access option.

[1]To whom correspondence should be addressed. Email: jlarsuaga@isciii.es.

This article contains supporting information online at www.pnas.org/lookup/suppl/doi:10.1073/pnas.1619040114/-/DCSupplemental.

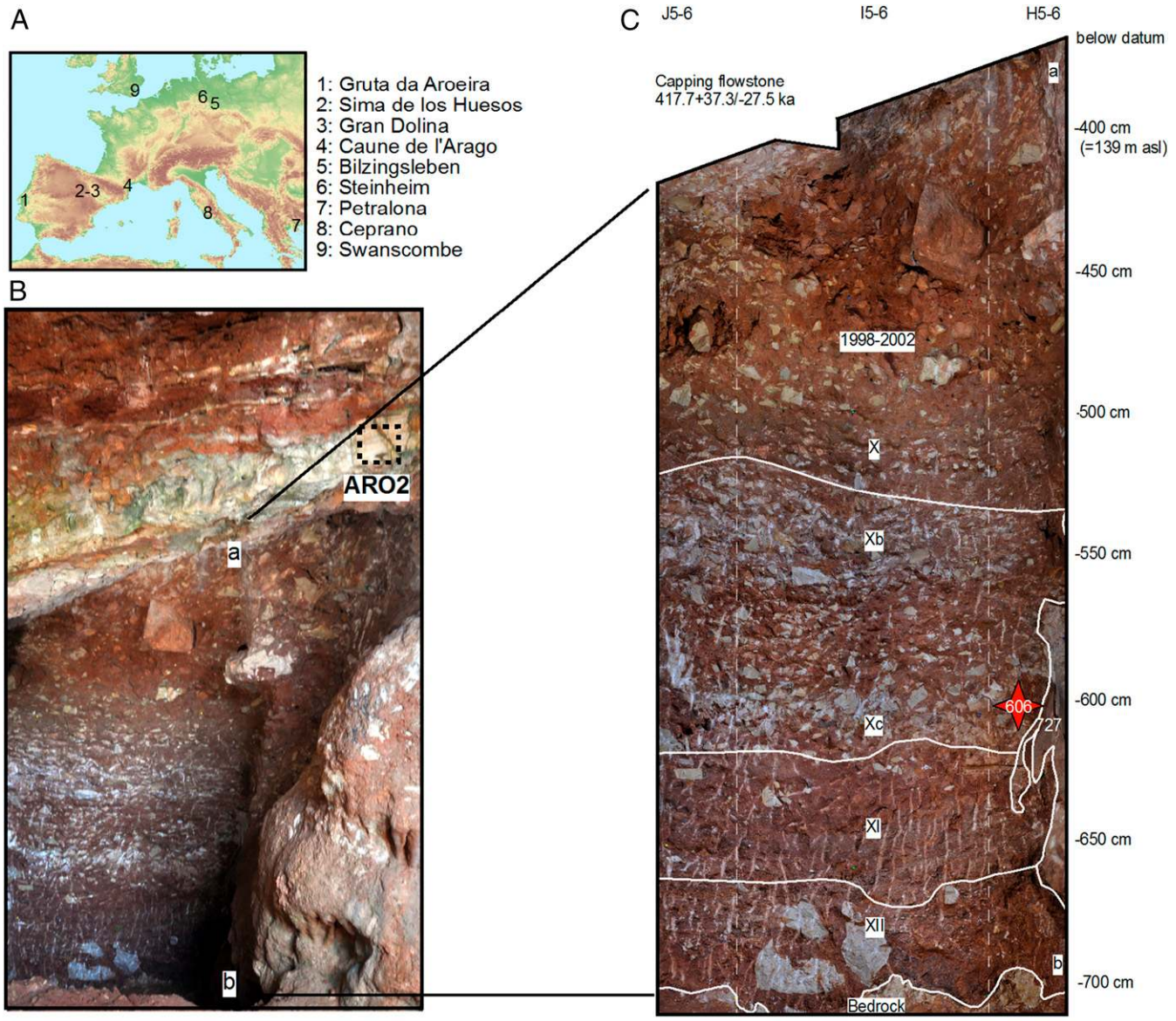

Fig. 1. (*A*) Geographical location of Gruta da Aroeira and main sites mentioned in the text. (*B*) Detail of the excavation area and provenance of the ARO2 U-series sample. (*C*) Stratigraphic profile and cranium provenance (denoted by its field inventory no. 606).

the raw material of choice, whereas flint is scarce, but both are represented among the handaxes (Fig. S2). The Levallois method is absent.

The faunal remains are highly fragmented, mainly consisting of isolated teeth, phalanges, carpal/tarsal bones, and antler fragments. Among the 209 piece-plotted faunal remains from layer X–Xb/c, cervids [number of identified specimens (NISP) = 58], including both *Dama* and *Cervus*, and equids (NISP = 46) predominate. Rarer species include Rhinocerotidae (NISP = 2) (likely *Stephanorhinus cf hundsheimensis*), and bear (NISP = 4) (*Ursus* sp.), as well as a large bovid (*Bos/Bison*), a caprid (Caprinae), and a tortoise (*Testudo* sp.) (NISP = 1 each). Several burnt bone fragments were recovered at the base of layer Xb/c in association with the stone tools and the human cranium.

The Aroeira 3 Cranium

Preservation. The Aroeira 3 cranium was painstakingly extracted from the hard calcareous breccia and restored (*SI In Situ Extraction of the Fossil* and Fig. S4). The cranium is taphonomically broken obliquely to the sagittal plane, with the preserved bone margin running diagonally from the left supraorbital arch anteriorly, crossing the midline just anterior to bregma, and continuing posteriorly toward the right asterion. Approximately half of the right parietal bone and the right half of the frontal bone are preserved. A circular portion of the right frontoparietal region was originally present but was destroyed in situ in the act of discovery (Fig. 3).

In addition, portions of the sphenoid and the nearly complete temporal bone are preserved, as well as the medial portion of the left supraorbital arch, the interorbital pillar (including the superior portions of both nasal bones), and most of the right supraorbital arch. The outer surface of the supraorbital torus is preserved only in the glabellar region and in the medial half of the right supraorbital arch (we use the term "supraorbital arch" to refer to the part of the supraorbital torus lateral to the glabellar region; thus, it comprises the supercilliary arch, the supraorbital margin, and the lateral trigone). In addition, a fragment of the right maxilla includes the lower border of the nasal aperture and a part of the anterior nasal floor. A small portion of the alveolar process of the right maxilla is also present, with two fragmentary molars partially preserved.

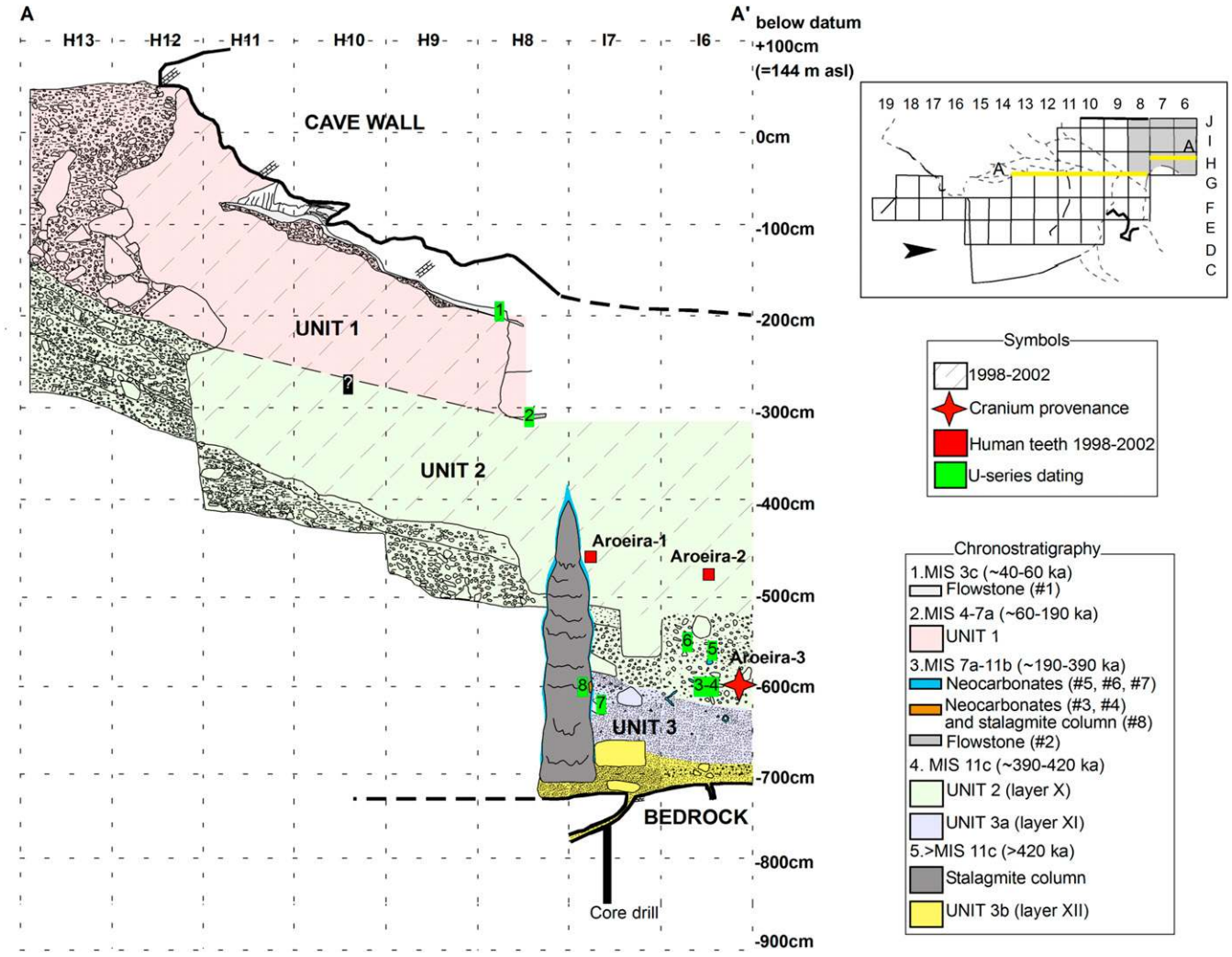

Fig. 2. Stratigraphic longitudinal profile of the Gruta da Aroeira, with the location of dating samples (nos.1–8) and human remains indicated. Dating samples are referred to in Table S1.

The cranial landmarks nasion, glabella, right asterion, right auriculare, and right porion are preserved. Although the bregma is not preserved, its position can be estimated accurately, because the coronal suture is preserved up to a point very close to the bregma. A remnant of the metopic suture is preserved near the glabella, as well as the right parietomastoid and occipitomastoid sutures and the segment of the lambdoid suture on the right parietal bone closer to the asterion. Internally, the frontal crest, foramen cecum, and crista galli are preserved in the anterior cranial fossa.

The coronal suture is fully fused, and there are no traces of the suture on the endocranial surface. In addition, the preserved teeth show fully formed roots, with closed apices, and the broken tooth crowns are worn flat. Although the enamel is present over nearly the entire preserved crown surface in both teeth, it is not possible to study the cusp pattern or details of occlusal anatomy, precluding a phylogenetic analysis of the dental morphology. Nevertheless, these observations collectively indicate an adult age for this individual.

Supraorbital Region. Two main supraorbital torus morphologies can be found in European Middle Pleistocene fossils. In many of them, the supraorbital arches are curved mediolaterally (in frontal view) and rounded on their anterior surface. The two arches can fuse completely in a swollen glabellar region (Fig. 3 and Fig. S5), or they can remain more or less separated in the midplane by a glabellar depression. This supraorbital morphology, with different degrees of glabellar fusion, is found in the large Atapuerca Sima de los Huesos (SH) sample, in the Bilzingsleben B1, Steinheim, and Petralona crania, and in the Late Pleistocene Neandertals (16). It is also seen in the Early Pleistocene Atapuerca Gran Dolina specimen ATD6-15. However, the Arago 21 and Ceprano specimens depart from this condition, resembling the Middle Pleistocene African specimens from Kabwe and Bodo in which the two supraorbital arches are well separated at the glabella and are flatter and less curved (17, 18). Despite the loss of the outer surface over much of the supraorbital torus, it is clear to us that the supraorbital arches in Aroeira 3 are fused in a swollen glabella (i.e., unlike the Ceprano and Arago 21 crania, the supraorbital torus in Aroeira 3 is not medially concave). Although the precise morphology of the supraorbital arches is more difficult to assess, the better-preserved right side seems to show a rounded condition, and the Bilzingsleben B1 specimen represents the closest Middle Pleistocene match to the Aroeira 3 supraorbital torus (Fig. S5).

Numerous Middle Pleistocene fossils, including the Kabwe, Bodo, Arago 21, and Petralona specimens (and perhaps the Steinheim specimen, although it has some deformation in this region) exhibit a nasion that is depressed with respect to glabella. In contrast, Neandertals and the Atapuerca (SH) sample show a nasion that projects

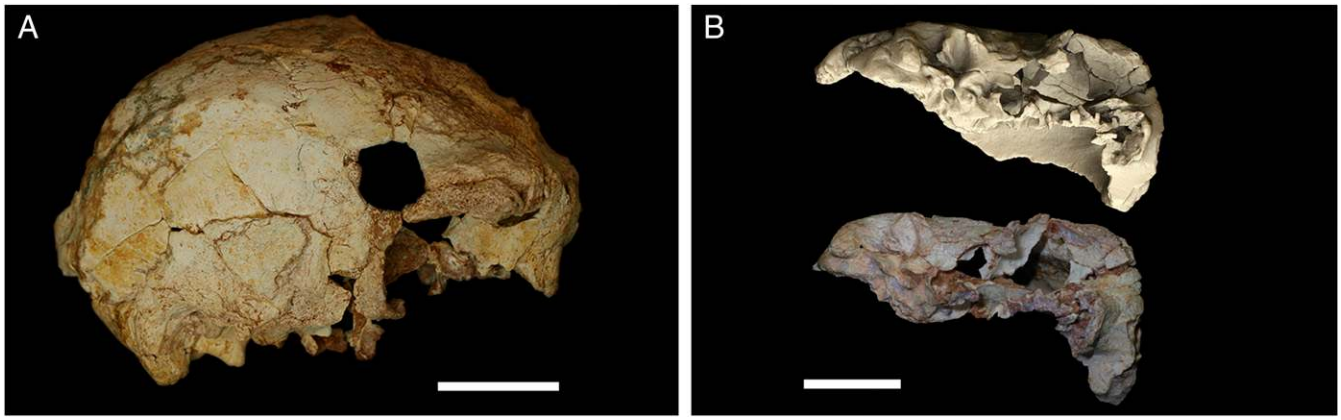

Fig. 3. The original completely restored Aroeira 3 cranium in lateral view (*A*) and the virtual reconstruction and original fossil in inferior view (*B*) (also see Figs. S4 and S5). (Scale bars, 5 cm.)

to the same degree as glabella. The Aroeira 3 cranium, like the Bilzingsleben B1 specimen, is intermediate in this trait (Figs. S5–S7).

Despite some abrasion of the outer surface, the right and left supraorbital arches are thick as compared with the majority of the European or African Middle or Late Pleistocene fossils (16, 19). The maximum midorbit thickness of the torus (19.0 mm) can be taken on the right side and is similar to that of the Bodo and Ceprano crania (each 17.5 mm), although the torus of the Bilzingsleben B1 cranium (21–22 mm, right side, cast measurement) is even thicker. The interorbital pillar is very broad. Although the dacryon and maxillofrontale landmarks cannot be located precisely, the distance between the two inner orbital borders is large (34–35 mm) and similar to the Atapuerca SH Cranium 4 (38.0 mm) and the Kabwe (32.0 mm), Bodo (37.5 mm), and Bilzingsleben B1 (35.5 mm, on cast) specimens. The frontal sinuses in the Aroeira 3 cranium are well developed (Fig. S7) but are not as large laterally (in the torus) or superiorly (in the frontal squama) as in the Petralona specimen.

Nasal Cavity. The lateral wall of the nasal cavity preserves the root of the inferior nasal concha as well as a sharp lateral nasal crest and a smooth turbinal crest (Fig. S3). An "internal nasal margin" (a "frame" made by the fusion of the turbinal and spinal crests) and a "medial projection" (bone swelling above the inferior nasal concha) described in Neandertals (20) are lacking in the Aroeira 3 cranium. This apparently derived internal nasal morphology in Neandertals is also absent in the Atapuerca (SH) sample but has been identified in the Steinheim cranium (20).

The nasal floor in the Aroeira 3 cranium is sufficiently preserved to determine that it is not bilevel. The Aroeira 3 cranium resembles the Gran Dolina and Sima de los Huesos hominins in showing a level or sloped configuration (the ancestral condition for *Homo*) but differs from the bilevel form present in most Late Pleistocene Neandertals and in the Steinheim, Petralona, east Asian archaic *Homo*, and some African Middle Pleistocene crania (21, 22).

Virtual Reconstruction. Virtual reconstruction of the Aroeira 3 cranium by mirror-imaging the right side (Fig. S5) shows that the parietal walls are nearly vertical. However, the maximum cranial breadth is located at the supramastoid crest, as in other earlier Middle Pleistocene European fossils. This morphology departs from the ancestral condition seen in *Homo erectus* of strongly convergent parietal walls superiorly and also from the more circular contour in posterior view of late Middle and Late Pleistocene Neandertals (16).

The auriculo-bregmatic height and frontal sagittal chord (with the bregma reconstructed) can be measured directly on the original fossil, and a number of bilateral measurements can be estimated in the virtual reconstruction (Table S2). Compared with the Atapuerca (SH) sample, the Aroeira 3 cranium is closer to Cranium 5 (1,090 cm^3) in the transverse diameters taken at both the auricular point and the supramastoid crest (i.e., on the temporal bone) and is intermediate or closer to Cranium 4 (1,390 cm^3) in the rest of the measurements. Thus, a cranial capacity above 1,100 cm^3 can safely be established.

Parietotemporal Region. An angular torus is present in the mastoid angle of the parietal bone in the Aroeira 3 cranium (Fig. S6). Among European Middle Pleistocene specimens, this feature is found only in a few large, robust individuals, including the Ceprano and Arago 47 crania and Atapuerca SH Cranium 4 (18, 23). In the Aroeira 3 cranium the parietal bone is ∼9 mm thick near the bregma and is 10.2 mm thick at the thickest point along the break (in the area of the parietal boss). These values are within the range of the Atapuerca (SH) sample. The thickness in the Aroeira 3 cranium near the asterion, at the angular torus, is large (14.6 mm) as it is in the other fossils that show this feature, including Atapuerca SH Cranium 4 (17.0 mm) and the Arago specimen (13.5 mm, on cast).

The temporal bone is nearly complete and preserves several phylogenetically relevant features. Although the squamosal portion is largely preserved, abrasion along the superior margin makes the height and curvature difficult to discern. The styloid process is fused to the basicranium, and there is a large and triangular postglenoid process. In both these features, the Aroeira cranium is different from Asian *H. erectus* but resembles the Atapuerca (SH) specimens (24). On the other hand, the articular eminence in the Aroeira 3 cranium is raised, unlike the derived flattened articular eminence in the Atapuerca (SH) crania, Steinheim and Petralona specimens and the Neandertals (25). The sphenoid bone contributes slightly to the medial wall of the glenoid fossa, but there is variation in this trait in the Atapuerca (SH) sample (24) and Neandertals. Other Neandertal derived features are also absent in the Aroeira 3 temporal bone, including an anterior bridge in the digastric groove or an external auditory meatus located at the same level as the zygomatic process root (26, 27).

In inferior view, the right mastoid process in the Aroeira 3 cranium projects well beyond the level of the occipitomastoid suture, whereas in most Neandertals the mastoid process characteristically does not project beyond the basicranium (24). Although different measurement techniques for mastoid projection have been proposed, we have measured the projection of the mastoid tip from the parietal incisure, because this measurement is not dependent on orienting the specimen in the Frankfurt horizontal orientation and has been found to differentiate Neandertals from other groups (25). When measured from the parietal incisure (Figs. S6 and S7), the mastoid projection in the Aroeira 3 cranium is low (33 mm), close to the Neandertal mean (36.4 ± 4.3) and to that of the Middle Pleistocene Steinheim specimen (31 mm, left side, on cast) and well below the range of values (40.0–50.0 mm) in the

Atapuerca (SH) sample (25). The digastric groove is deep and lacks a paramastoid crest (a bony ridge located between the mastoid process and the occipitomastoid suture, sometimes called the "juxtamastoid eminence"), but there is variation of this feature in modern and fossil populations, including the Atapuerca (SH) sample.

Internally, the transverse sulcus crosses the parietal bone above the asterion before entering the temporal bone (Fig. S5). This condition is observed in modern humans and some Neandertal specimens, but the transverse sulcus generally does not cross the parietal bone in earlier hominins, including the Atapuerca (SH) sample (16, 28).

Discussion

Most researchers support a European origin and a local evolution for the Neandertals (23, 29–31). However, despite the relatively good fossil record of Neandertals and their recently sequenced nuclear genome (32, 33), considerable debate still exists regarding the time of divergence of the lineages leading to modern humans and Neandertals and regarding the name, hypodigm, and geographic distribution of the stem species. One of the main reasons for this ongoing debate is the scarcity, generally fragmentary preservation, and often unclear chronology of most European Middle Pleistocene fossils, and the taxonomic classification of many of these Middle Pleistocene European fossils (as well as those from Africa and Asia) remains controversial (23, 31, 34–37).

At present three different cranial morphologies can be recognized in the European Middle Pleistocene hominin record. One is almost fully Neandertal, with nearly the entire suite of derived traits, and occurs during the last part of this period, mainly <200 ka. A second cranial configuration shows many Neandertal traits in the face, supraorbital torus, temporal bone, and mandible, but the general shape of the neurocranium (in both lateral and posterior views) is not Neandertal-like, indicating a mosaic nature for Neandertal cranial evolution.

The Atapuerca (SH) sample conforms to this cranial morphology (23), and ancient DNA analysis has shown that the Atapuerca (SH) hominins are members of the Neandertal clade (38). The incomplete braincase from Swanscombe should probably be grouped with the Atapuerca (SH) hominins as well, even though it is more Neandertal-derived in its excavated suprainiac area and its bilaterally projecting occipital torus. The Swanscombe specimen is dated to MIS 11 (29), and the Atapuerca (SH) sample is dated to MIS 11 or MIS 12 (39). The supraorbital morphology, especially in the glabellar region, where it is better preserved, and the mastoid process projection may indicate that the Aroeira 3 cranium (dated to MIS 11) also belongs in this category, even though the combination of traits is not the same as in the Atapuerca (SH) crania or any other fossil in this group.

Finally, there are other European partial crania, such as the Arago 21 and Ceprano specimens, that do not show Neandertal-derived traits in the preserved regions or in which the features are more ambiguous (36). The Aroeira 3 cranium resembles these specimens in its well-developed angular torus (also present in Atapuerca SH Cranium 4) and its lack of a flattened articular eminence.

Although the taxonomic identity of the Arago and Ceprano hominins is debated, some authors prefer to group them with other Middle Pleistocene fossils from Africa and Asia in a separate species (*Homo heidelbergensis*) (34, 40). This view sees the Neandertals as evolving out of *H. heidelbergensis* in Europe and posits a largely anagenetic (linear) evolutionary scenario. Other researchers (23) have argued for a high degree of morphological diversity in the Middle Pleistocene European hominin record, a scenario that is incompatible with an anagenetic evolutionary pattern. Evolutionary scenarios that posit a series of temporally successive grade shifts are likely to be largely a product of the general paucity and poor chronological control of the European Middle Pleistocene fossil record. Elucidating nonlinear evolutionary patterns in the hominin fossil record relies on fossil morphology, as well as geography and chronology, and the addition of relatively complete, well-dated fossils, such as the Aroeira 3 specimen, will help establish a more robust evolutionary scenario.

Conclusions

The Aroeira 3 cranium shows several features characteristic of European earlier Middle Pleistocene crania. However, the combination of traits in the Aroeira 3 cranium is not seen in any other Middle Pleistocene individual. The Aroeira 3 cranium shows a continuous and thick supraorbital torus similar to that of the Bilzingsleben cranium, a short mastoid process as in the Steinheim specimen, and a large, triangular postglenoid process as in the Atapuerca (SH) sample. These features are combined with a raised articular eminence, which contrasts with the flatter articular eminence generally seen in the Atapuerca (SH) sample and in the Steinheim cranium. It has been argued that a flattened articular eminence is a feature that appears very early in Neandertal evolution (23, 41).

The Aroeira, Atapuerca (SH), and Arago sites are relatively close to one another in time (400–450 ka) and space (southwestern Europe), but the fossils from these sites are clearly different. These differences suggest that intra- or interdeme hominin diversity and complex population dynamics characterized this period, including variable population replacement with varying levels of isolation and admixture (23). In fact, it has been argued that archaic paleodemes (e.g., Ceprano) could have persisted in ecogeographic refugia (36) along with more evolved paleodemes (e.g., Atapuerca Sima de los Huesos) showing Neandertal apomorphies in other regions. This same time period also documents two major technological innovations: the expansion of the Acheulean tradition (42) and the first evidence for widespread, systematic controlled use of fire (43). Both are present at the Aroeira site, whose geographic situation in extreme southwestern Europe suggests that these innovations spread quickly throughout the European continent and were largely independent of hominin morphological diversity [although with the arrival of the Acheulean industry to Western Europe, the possibility of gene flow from outside Europe should also be taken into account (38)]. Well-dated fossils, such as the Aroeira 3 cranium, with a clear technological and ecological context are crucial to building a robust evolutionary scenario during the European Middle Pleistocene.

Materials and Methods

U-Th Dating Samples and Sample Preparation. U-Th dating was carried out on eight speleothem specimens found in stratigraphic relationship with the excavated units or the cranium itself (Table S1). We dated flowstones ARO1 and ARO2, which were capping units 1 and 2, respectively, and a basal section of a stalagmite (BL1), which formed over the flowstone that caps the Pleistocene fill exteriorly, at the Brecha das Lascas locus (Figs. 1 and 2). Results for these samples were presented and discussed in ref. 9. For the present study, we dated two additional calcite crystals which precipitated inside sediment voids of unit 2 (ARO14-03 and ARO14-04) (Table S1), providing a minimum age for the sediment accumulation. We furthermore analyzed the outer layer and a postsedimentation overgrowth of a stalagmitic column (ARO14-H6-727) covered by unit 2. We finally analyzed two calcite crusts (ARO-SK4 and ARO-SK6) that precipitated on the Aroeira 3 cranium, providing minimum ages for the specimen (Table S1). Subsamples were cut from the collected specimen using a microdrill fitted with a diamond cutting disk. The $CaCO_3$ pieces were cleaned in an ultrasound bath and dried. Chemical separation and purification was done following previously described protocols (44). Purified U and Th fractions were analyzed in 0.5 M HCl solution by multicollector-inductively coupled plasma mass spectroscopy (MC-ICPMS). Analytical protocols for MC-ICPMS and data reduction are presented in detail in ref. 45.

Conservation and Restoration of the Aroeira Cranium. The conservation process in the laboratory consisted of extracting the cranium from the breccia and adhering speleothem coating and cleaning and removing sediment and limestone pebbles between the fossil and the speleothem. This cleaning was done using two different types of drills with different steel bits and ultrasound techniques. After cleaning, the fragments were joined together using an acrylic resin adhesive, Paraloid B-72 (Rohm & Haas), at 15–30% acetone concentration (Fig. S4) (46). Once the fossil was reconstructed, a final thin layer of consolidant Paraloid B-72 (Rohm & Haas) at 3% acetone concentration was applied to the entire surface. Endocranially, a thin layer of possible speleothem remains coating the superior portion of the petrous pyramid (Fig. S4), because the benefits of removal were outweighed by possible damage to the fossil.

CT Scanning and Virtual Reconstruction. The Aroeira 3 cranium was subjected to high-resolution CT scanning using a YXLON MU 2000-CT scanner housed at the University of Burgos, Burgos, Spain, with the following scanning parameters: 160 kV, 4 mA, 0.5-mm slice thickness, 0.3-mm interslice distance, and a field of view of 221.88 mm. Six hundred twelve slices were obtained as a 1,024 × 1,024 matrix of 32-bit Float format with a final pixel size of 0.162 mm. Virtual reconstruction of the cranium (Fig. S5), relying on mirror-imaging across the sagittal plane, was carried out using the Mimics v.18 (Materialise, N.V.) software program. The virtual reconstruction initially aligned the two halves of the cranium relying on the recognition of homologous landmarks. Subsequently, a "best fit" of the overlapping mesh surfaces, consisting of 500,000 triangles, was carried out relying on ∼50 automated iterations. Because of the lack of direct contact, no attempt was made to situate the maxillary fragments with respect to the cranial vault.

ACKNOWLEDGMENTS. We thank J. Trueba for photographic documentation of the restored cranium. CT scanning of the Aroeira 3 cranium was carried out at the University of Burgos Scientific Park by R. Porres and in collaboration with J. M. Carretero and L. Rodríguez from the Laboratory of Human Evolution at University of Burgos. This research was supported by the Ministerio de Economía y Competitividad of the Government of Spain, Projects HAR2014-55131, CGL2012-38434-C03-01, and CGL2015-65387-C3-2-P (MINECO/FEDER). Fieldwork was funded by Câmara Municipal de Torres Novas and Fundação para a Ciência e Tecnologia with logistical support by Fábrica de Papel A Renova. J.D. was supported by Postdoctoral Grant SFRH/BPD/100507/2014 from the Portuguese Fundação para a Ciência e a Tecnologia using funding from the European Social Fund/Operational Programme for Human Potential, and M.S was supported by Juan de la Cierva Postdoctoral Grant FJCI-2014-21386.

1. Zilhão J, et al. (2010) Humans and hyenas in the Middle Paleolithic of Gruta da Oliveira (Almonda karstic system, Torres Novas, Portugal). *1a Reunión de Científicos sobre Cubiles de Hiena (y Otros Grandes Carnívoros) en los Yacimientos Arqueológicos de la Península Ibérica*, Zona Arqueológica, eds Baquedano E, Rosell J (Museo Arqueológico Regional, Alcala de Henares, Spain) Vol. 13, pp 298–308.
2. Zilhão J, Maurício J, Souto P (1991) A arqueologia da Gruta do Almonda (Torres Novas). Resultados das escavações de 1988-89. *Actas das IV Jornadas Arqueológicas* (Associação dos Arqueólogos Portugueses, Lisbon), pp 161–166.
3. Zilhão J, Maurício J, Souto P (1993) Jazidas arqueológicas do sistema cársico da nascente do Almonda. *Nova Augusta* 7:35–54.
4. Trinkaus E, Bailey S, Davis S, Zilhão J (2011) The Magdalenian human remains from the Galeria da Cisterna (Almonda karstic system, Torres Novas, Portugal) and their archeological context. *O Arqueólogo Português* 5(1):395–413.
5. Trinkaus E, Maki J, Zilhão J (2007) Middle Paleolithic human remains from the Gruta da Oliveira (Torres Novas), Portugal. *Am J Phys Anthropol* 134(2):263–273.
6. Trinkaus E, et al. (2003) Later Middle Pleistocene human remains from the Almonda Karstic system, Torres Novas, Portugal. *J Hum Evol* 45(3):219–226.
7. Angelucci DE, Zilhão J (2009) Stratigraphy and formation processes of the Upper Pleistocene deposit at Gruta da Oliveira, Almonda karstic system, Torres Novas, Portugal. *Geoarchaeology* 24(3):277–310.
8. Willman JC, Maki J, Bayle P, Trinkaus E, Zilhão J (2012) Middle Paleolithic human remains from the Gruta da Oliveira (Torres Novas), Portugal. *Am J Phys Anthropol* 149(1):39–51.
9. Hoffmann DL, Pike AW, Wainer K, Zilhão J (2013) New U-series results for the speleogenesis and the Palaeolithic archaeology of the Almonda karstic system (Torres Novas, Portugal). *Quat Int* 294:168–182.
10. Richter D, et al. (2014) Heated flint TL-dating for Gruta da Oliveira (Portugal): Dosimetric challenges and comparison of chronometric data. *J Archaeol Sci* 41:705–715.
11. Gameiro C, Aubry T, Almeida F (2008) L'exploitation des matières premières lithiques au Magdalénien final en Estremadure Portugaise: Données sur les sites de Lapa dos Coelhos et de l'abri 1 de Vale dos Covões. *Space and Time: Which Diachronies, Which Synchronies, Which Scales*, British Archaeological Reports International Series, eds Aubry T, Almeida F, Araujo A, Tiffagom M (Archeopress, Oxford, UK), pp 57–67.
12. Zilhão J, et al. (2013) A Gruta da Oliveira (Torres Novas): Uma jazida de referência para o Paleolítico Médio da Península Ibérica. *Arqueologia em Portugal-150 anos*, eds Arnaud J, Martins A, Neves C (Associação dos Arqueólogos Portugueses, Lisbon), pp 259–268.
13. Marks A, et al. (2002) Le gisement Pléistocène moyen de Galeria Pesada, (Estrémadure, Portugal): Premiers résultats. *Paléo* 14:77–100.
14. Trinkaus E (2004) Dental crown dimensions of Middle and Late Pleistocene European humans. *Misceánea en Homenaje a Emiliano Aguirre III: Paleoantropología*, ed Rubio S (Museo Arqueológico Regional, Alcalá de Henares, Spain), pp 393–398.
15. Martinón-Torres M, Bermúdez de Castro JM, Gómez-Robles A, Prado-Simón L, Arsuaga JL (2012) Morphological description and comparison of the dental remains from Atapuerca-Sima de los Huesos site (Spain). *J Hum Evol* 62(1):7–58.
16. Arsuaga JL, Martínez I, Gracia A, Lorenzo C (1997) The Sima de los Huesos crania (Sierra de Atapuerca, Spain). A comparative study. *J Hum Evol* 33(2-3):219–281.
17. Rightmire GP (1996) The human cranium from Bodo, Ethiopia: Evidence for speciation in the Middle Pleistocene? *J Hum Evol* 31(1):21–39.
18. Manzi G, Mallegni F, Ascenzi A (2001) A cranium for the earliest Europeans: Phylogenetic position of the hominid from Ceprano, Italy. *Proc Natl Acad Sci USA* 98(17):10011–10016.
19. Smith FH, Ranyard GC (1980) Evolution of the supraorbital region in Upper Pleistocene fossil hominids from South-Central Europe. *Am J Phys Anthropol* 53(4):589–610.
20. Schwartz JH, Tattersall I, Teschler-Nicola M (2008) Architecture of the nasal complex in Neanderthals: Comparison with other hominids and phylogenetic significance. *Anat Rec (Hoboken)* 291(11):1517–1534.
21. Franciscus RG (2003) Internal nasal floor configuration in *Homo* with special reference to the evolution of Neandertal facial form. *J Hum Evol* 44(6):701–729.
22. Wu X-J, Maddux SD, Pan L, Trinkaus E (2012) Nasal floor variation among eastern Eurasian Pleistocene *Homo*. *Anthropol Sci* 120(3):217–226.
23. Arsuaga JL, et al. (2014) Neandertal roots: Cranial and chronological evidence from Sima de los Huesos. *Science* 344(6190):1358–1363.
24. Martínez I, Arsuaga JL (1997) The temporal bones from Sima de los Huesos Middle Pleistocene site (Sierra de Atapuerca, Spain). A phylogenetic approach. *J Hum Evol* 33(2-3):283–318.
25. Martínez I, Quam R, Arsuaga J (2008) Evolutionary trends in the temporal bone in the Neandertal lineage: A comparative study between the Sima de los Huesos (Sierra de Atapuerca) and Krapina samples. *New Insights on the Krapina Neandertals: 100 Years After Gorjanović-Kramberger*, eds Monge J, Mann A, Frayer D, Radovčić J (Croatian Natural History Museum, Zagreb, Croatia), pp 75–80.
26. Trinkaus E (1983) *The Shanidar Neandertals* (Academic, New York).
27. Hublin JJ (1988) Caractères dérivés de la région occipito-mastoïdienne chez les néandertaliens. *L'Homme de Néandertal, 3: L'Anatomie*, ed Trinkaus E (Études et Recherches Archéologiques de l'Université de Liège, Liege, France), pp 67–73.
28. Arsuaga JL, et al. (1989) The human remains from Cova Negra (Valencia, Spain) and their place in European Pleistocene human evolution. *J Hum Evol* 18:55–92.
29. Stringer C (2011) The changing landscapes of the earliest human occupation of Britain and Europe. *The Ancient Human Occupation of Britain*, eds Ashton N, Lewis S, Stringer C (Elsevier, Amsterdam), pp 1–10.
30. Dean D, Hublin JJ, Holloway R, Ziegler R (1998) On the phylogenetic position of the pre-Neandertal specimen from Reilingen, Germany. *J Hum Evol* 34(5):485–508.
31. Hublin JJ (2009) The origin of Neandertals. *Proc Natl Acad Sci USA* 106(38): 16022–16027.
32. Green RE, et al. (2010) A draft sequence of the Neandertal genome. *Science* 328(5979):710–722.
33. Prüfer K, et al. (2014) The complete genome sequence of a Neanderthal from the Altai Mountains. *Nature* 505(7481):43–49.
34. Rightmire GP (2008) *Homo* in the Middle Pleistocene: Hypodigms, variation, and species recognition. *Evol Anthropol* 17(1):8–21.
35. Manzi G (2016) Humans of the Middle Pleistocene: The controversial calvarium from Ceprano (Italy) and its significance for the origin and variability of *Homo heidelbergensis*. *Quat Int* 411:254–261.
36. Manzi G, Magri D, Palombo MR (2011) Early–Middle Pleistocene environmental changes and human evolution in the Italian peninsula. *Quat Sci Rev* 30(11):1420–1438.
37. de Lumley M-A (2015) L'homme de Tautavel. Un *Homo erectus* européen évolué. *Homo erectus tautavelensis*. *Anthropologie* 119(3):303–348.
38. Meyer M, et al. (2016) Nuclear DNA sequences from the Middle Pleistocene Sima de los Huesos hominins. *Nature* 531(7595):504–507.
39. Arnold LJ, et al. (2014) Luminescence dating and palaeomagnetic age constraint on hominins from Sima de los Huesos, Atapuerca, Spain. *J Hum Evol* 67:85–107.
40. Stringer C (2012) The status of *Homo heidelbergensis* (Schoetensack 1908). *Evol Anthropol* 21(3):101–107.
41. Falguères C, et al. (2015) New ESR and U-series dating at Caune de l'Arago, France: A key-site for European Middle Pleistocene. *Quat Geochronol* 30(B):547–553.
42. Santonja M, Villa P (2006) The Acheulian of Western Europe. *Axe age: Acheulian Tool-Making from Quarry to Discard*, eds Goren-Inbar N, Sharon G (Equinox, London), pp 429–478.
43. Roebroeks W, Villa P (2011) On the earliest evidence for habitual use of fire in Europe. *Proc Natl Acad Sci USA* 108(13):5209–5214.
44. Hoffmann DL, Pike AW, García-Diez M, Pettitt PB, Zilhão J (2016) Methods for U-series dating of $CaCO_3$ crusts associated with Palaeolithic cave art and application to Iberian sites. *Quat Geochronol* 36:104–119.
45. Hoffmann DL, et al. (2007) Procedures for accurate U and Th isotope measurements by high precision MC-ICPMS. *Int J Mass Spectrom* 264(2):97–109.
46. Ortega MC, et al. (2009) Restauration d'un fémur fossile humain du site de la Sima de los Huesos (Atapuerca, Espagne). *Anthropologie* 113(1):233–244.
47. Davidson A, Brown G (2012) Paraloid TM B-72: Practical tips for the vertebrate fossil preparator. *Collection Forum* 26:99–119.
48. Davidson A, Alderson S (2009) An introduction to solution and reaction adhesives for fossil preparation. *Methods in Fossil Preparation: Proceedings of the First Annual Fossil Preparation and Collections Symposium*, pp 53–62.
49. Down J, MacDonald MJT, Williams R (1996) Pruebas de adhesivos en el Canadian Conservation Institute. Una evaluación de una selección de adhesivos acrílicos y de acetato de polvinilo. *Cuadernos de Conservación* 41(1):12–21.
50. International Council of Museums Committee for Conservation (2008) *Terminology to Characterize the Conservation of Tangible Cultural Heritage*. (ICOM-CC; New Delhi, India).
51. International Council on Monuments and Sites (2013) The Australia ICOMOS charter for the conservation of places of cultural significance (the Burra charter). (Australia ICOMOS, Canberra, Australia).
52. Jaffey A, Flynn K, Glendenin L, Bentley W, Essling A (1971) Precision measurement of half-lives and specific activities of U 235 and U 238. *Phys Rev C Nucl Phys* 4(5):1889–1906.
53. Cheng H, et al. (2000) The half-lives of uranium-234 and thorium-230. *Chem Geol* 169(1):17–33.
54. Holden NE (1990) Total half-lives for selected nuclides. *Pure Appl Chem* 62(5):941–958.
55. Bräuer G (1988) Osteometrie. *Anthropologie*. ed Knussmann R (G. Fischer, Stuttgart), Vol 1, Part 1, pp 160–232.
56. Howells W (1973) *Cranial Variation in Man: A Study by Multivariate Analysis of Patterns of Difference Among Recent Human Populations*. Papers of the Peabody Museum of Archaeology and Ethnology (The Peabody Museum of Archaeology and Ethnology, Harvard University: Cambridge, MA), Vol 67.